Assiut University Journal of Multidisciplinary Scientific Research (AUNJMSR)
Faculty of Science, Assiut University, Assiut, Egypt.
Printed ISSN 2812-5029
Online ISSN 2812-5037
Vol. 54(1): 65- 85 (2025)
https://aunj.journals.ekb.eg

Geophysical investigation to anticipate the groundwater aquifers interconnection from Sohag to Assiut Governorates, Upper Egypt

Ibrahim A. Ibrahim1, *, Abotalib Z. Abotalib2,3, Haby S. Mohamed1, Mahmoud M. Senosy1

[1]Geology Department, Faculty of Science, Assiut University, Assiut, Egypt

[2]Division of Geological Applications and Mineral Resources, National Authority for Remote Sensing and Space Sciences, Cairo, Egypt

[3]National Center for Environmental Compliance, Riyadh, Saudi Arabia

[*]Corresponding Author: ibrahimaboasem@science.aun.edu.eg

ARTICLE INFO

Article History:
Received: 2024-07-28
Accepted: 2024-10-20
Online: 2024-12-26

Keywords:
Groundwater aquifers interconnection, Nubian Sandstone Aquifer System (NSAS), Carbonate Aquifer System (CAS), aeromagnetic data, Upper Egypt.

ABSTRACT

Investigating groundwater resources in Egypt is crucial, particularly in light of the water scarcity issues in this hyper-arid region and the ongoing climatic challenges. The replenishment of shallow aquifers by deep mega aquifers is significant because it supports the heavily utilized and easily accessible shallow aquifers. This replenishment occurs via vertical and sub-vertical faults. In this study aeromagnetic data were utilized to reveal subsurface deep-seated major faults and to infer their relation to major surface faults that were traced from the published geological maps of Egypt. The analysis and interpretation of the present data revealed that the main subsurface structural trend is extending NE-SW, while the main surface fault trend runs in an opposite position extending NW-SE. This discrepancy in the extension of surface and subsurface faults indicates lack of a vertical and/or

subvertical continuity. Consequently, no interconnection exists between the deep Nubian Sandstone Aquifer System (NSAS) and the shallow Carbonate Aquifer System (CAS), implying no upward feeding from the NSAS towards the CAS in the study area. This anticipation is confirmed from the stable isotopic analyses for some representing groundwater samples which were carried out and published in a literature.

1. INTRODUCTION

Geophysical investigations are crucial in groundwater evaluation, offering a spatially extensive, non-invasive approach to explore the subsurface geology and address the groundwater potentiality [1]. Among various geophysical techniques, magnetic methods are particularly of notable capacity to detect subsurface structures that can function as conduits or barriers to groundwater flow [2, 3].

Comprehending the hydrogeological connection between aquifers is essential for sustainable water resource management, especially in regions experiencing water scarcity. This connection involves the movement of water across aquifers, which is influenced by geological, hydrological, and anthropogenic factors [4, 5]. Understanding these interactions is crucial for effective groundwater management and for mitigating issues related to water availability and quality in affected areas [6].

Faults can either facilitate or obstruct the groundwater flow, depending on their specific characteristics. Thus, faults can serve as conduits or barriers to the groundwater movement and, consequently, can greatly affect the vertical connectivity between aquifers [7]. A thorough understanding of how faults influence vertical groundwater flow is essential for effective groundwater management, especially in regions with complex geological settings and multiple aquifer systems [7, 8]. The hydrogeological connectivity between aquifers can occur vertically and sub-vertically through faults and fractures, enabling water to bypass confining layers and move between aquifers [9]. In addition, a multi-component hydro-geochemical technique must be applied to investigate how deep thermal fluids rise into shallow aquifers; such phenomenon was studied in the Contursi region of Italy [10].

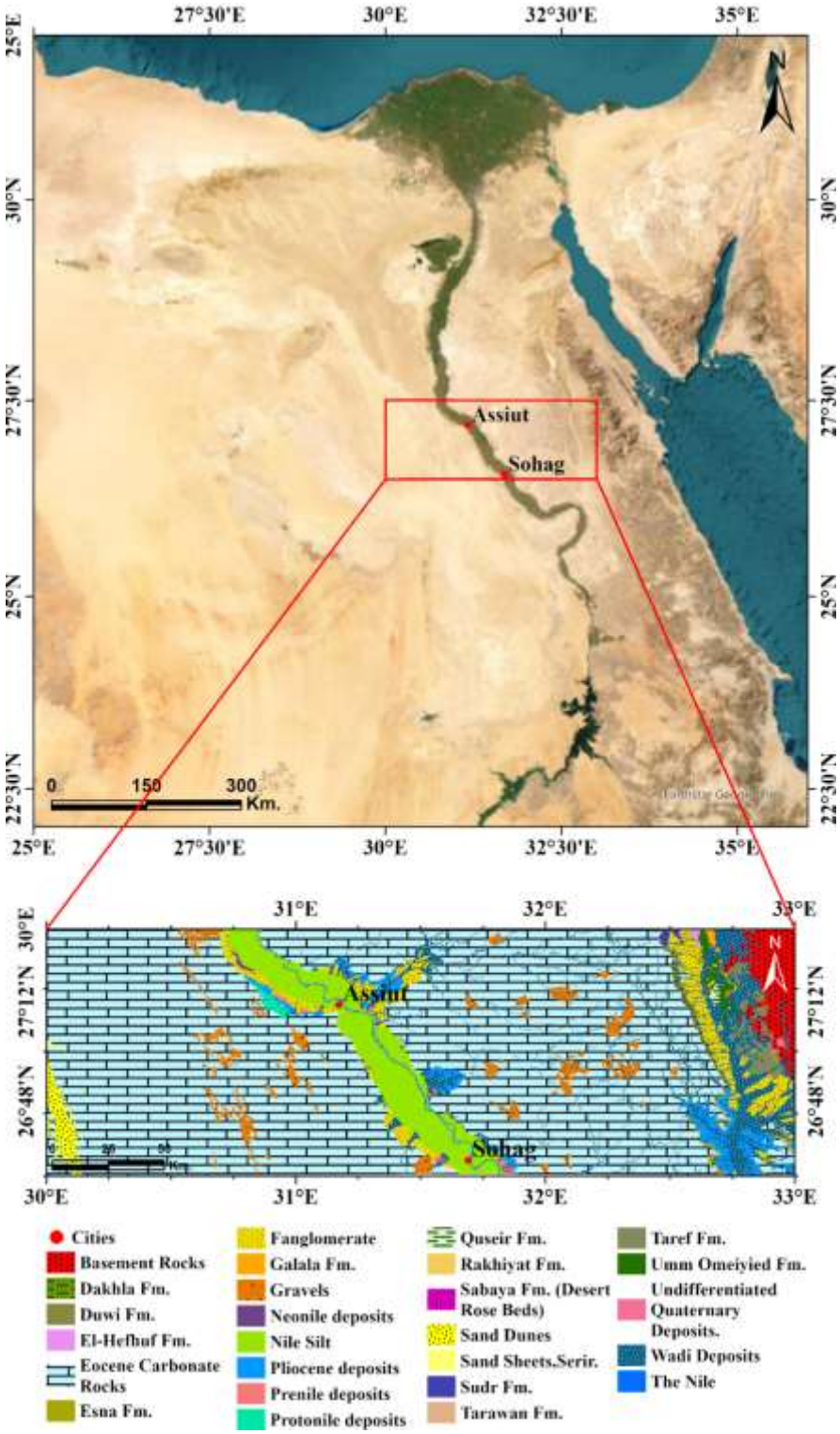

Fig. 1: A) Location map showing the area between Sohag and Assiut Governorates, B) Geological map of the study area and its east-west surroundings, showing the exposed Pre-Cambrian (basement) to Eocene rock units, after [11].

The present study area extends from 30° to 33° E and from 26.5° to 27.5° N (figure 1A). This study aims to predict the connection status between the deep Nubian Sandstone Aquifer System (NSAS) and the shallow Carbonate Aquifer System (CAS) from Sohag to Assiut Governorates (the Western border), Upper Egypt. This investigation is accomplished through analyzing aeromagnetic data prepared by the Egyptian General Petroleum Corporation in 1989 (scale 1:500,000). The major surface faults are traced from the geological map of Egypt (scale 1:2,000,000) published by the Egypt Geological Survey and Minning Authority in 1981. The deep subsurface faults are correlated to the surface faults obtained from geological map to examine their continuity from the surface to the subsurface.

2. SURFACE OUTCROPS IN THE STUDY AREA

The dominant succession in the study area (figure 1B) is the early-late Lower Eocene marine sedimentary rocks. These sediments form huge thicknesses of various limestones, constituting the Thebes Group [12]. These rocks overlay Campanian-Maastrichtian shallow to deep marine sediments, which belong to the Quseir (base), Duwi and Dakhla formations. The Quseir Formation is composed predominantly of phosphorite beds interbedded with shales, marls, and some limestone while the Duwi Formation features extensive phosphorite deposits, along with shales, marls, and limestone. The Dakhla Formation consists mainly of dark shales, marls, and some limestone, indicating a deeper marine setting [13].

3. HYDROGEOLOGICAL SETTING

3.1. The Nubian Sandstone Aquifer System (NSAS)

The Nubian Sandstone Aquifer System (NSAS) is one of the world's largest and most important fossil aquifer systems. It extends across Egypt, Libya, Sudan, and Chad, and is considered a critical water resource aquifer, particularly in such arid regions where surface water is scarce. The NSAS consists predominantly of sandstone that date back to the Paleozoic and Mesozoic. In Egypt, the Nubian Sandstone is characterized by its high porosity and permeability [14]. The NSAS is a vast, multi-layered aquifer system, with individual sandstone layers, acting mostly as confined aquifers. Groundwater within this aquifer is typically ancient, having been recharged during wetter climatic periods thousands years ago. Its aquifer system reflects

significant variations in depth and thickness across different regions, influencing therefore the availability and quality of groundwater [15].

3.2. The Carbonate Aquifer System (CAS):

This aquifer system is characterized by its extensive carbonate rock formations, which store significant amounts of groundwater. These carbonate rocks are highly porous and permeable, allowing substantial groundwater storage and flow. The aquifer system is predominantly unconfined to semi-confined, depending on the overlying sediments and geological structures. The groundwater flow is influenced by the regional hydraulic gradient, which generally flows from the Western Desert towards the Nile Valley [16]. The main rock units that constitute the CAS are the Eocene limestones, which form the primary aquifer unit, and the Miocene limestones that overlay the Eocene limestones, contributing also to the aquifer system. It is characterized by more heterogeneous lithologies, including limestones, dolostones, and occasional evaporites [17].

4. MATERIALS AND METHODS

The reduced-to-pole aeromagnetic maps that cover the study area with an original scale 1: 500,000 and represents part of the aeromagnetic survey of Egypt were used in this work. These maps were carried out for the Egyptian General Petroleum Corporation by Aero Service Division, Western Atlas International Incorporation, the United States Agency for International Development, released in 1989, with contour interval of 25 nT. The used sheet is reduced to pole because it is an important advantage to reduce the magnetic field to the north magnetic pole. The magnetic interpretation can be complicated by the fact that the magnetic anomalies, associating different geologic bodies, change their configuration as the inclination of the earth's magnetic field changes [18]. The geological maps produced by Conoco Coral Corporation in 1987 in cooperation with the Egyptian General Petroleum Corporation were incorporated in the investigation to display the geological formations of the study area [11]. In order to trace the major surface faults in the study area, the geologic map of Egypt produced by the Egyptian Geological Survey and Minning Authority [19] is used.

The processing software Geosoft Oasis Montaj v8.4 [20] was mainly applied to process the collected aeromagnetic data. The methodology applied for this research encompasses the processing and interpretation of the aeromagnetic data to identify and analyze significant

concealed subsurface faults. The resulting fault trends were correlated with major surface faults identified from geological maps. In the following section, a brief description of the filters and interpretation techniques, which applied to the reduced-to-pole aeromagnetic data, is given.

5. PROCESSING OF THE AEROMAGNETIC DATA

5.1. Upward continuation:

The upward continuation filter refines magnetic data by revealing deeper features, throughout suppressing the influence of the shallow anomalies and highlighting the signals of the deeper sources within the Earth. This discrimination between shallow and deep features is crucial for successful subsurface exploration [22]. It is used to get rid of the surface noise imprinted on the data. This concept grants smooth processing operations and filtering that focus primarily on the deep subsurface features, not on the shallow ones. The mathematical expression in the wavenumber domain of this filter is expressed by equation (1) as follows:

$$\mathbf{L(k) = e^{-2\pi hk}} \quad (\mathbf{1})$$

Where, k is the wavenumber domain increment, used to depict a radially symmetrical variable and h is the distance in ground units, relative to the plane of observation to continue upward.

5.2. First Vertical derivative (FVD):

It enhances the resolution of the shallow magnetic anomalies and assists in delineating the subsurface geological features more precisely. This is done by highlighting the edges and boundaries of magnetic sources; the first vertical derivative of a magnetic field measures the rate of change of the magnetic field with respect to the vertical direction [23]. The First Vertical Derivative (FVD) is given via formula (2) as follows:

$$\mathbf{FVD} = \frac{\mathbf{dT}}{\mathbf{dz}} \quad (\mathbf{2})$$

Where T is the total magnetic field.

5.3. Butterworth high pass filter:

This filter is intended to eliminate the low-frequency components of the signal, thereby highlighting higher-frequency anomalies linked to near-surface geological features. It offers a smooth and effective procedure to accentuate the higher-frequency elements while reducing undesirable low-frequency noise [24]. Equation (3) shows the mathematical formula of this filter.

$$\mathbf{L(k)} = \frac{\frac{\mathbf{k}}{\mathbf{k_c}}}{\left[\mathbf{1}+\left(\frac{\mathbf{k}}{\mathbf{k_c}}\right)^{\mathbf{n}}\right]} \quad \mathbf{(3)}$$

Where, k is the wavenumber domain increment, k_c is the inflection point of the wavenumber cutoff in cycles/ground unit and n is a positive integer value determining the degree of sharpness of the cutoff.

5.4. Analytic Signal (AS):

The analytic signal is determined by taking the square root of the sum of the squares of the vertical derivative and the two horizontal derivatives of the total field. This technique is effective in identifying the edges of the magnetic source bodies [25]. Equation (4) displays the mathematical formula for the AS as follows:

$$\mathbf{AS} = \sqrt{\left(\frac{\mathbf{dT}}{\mathbf{dx}}\right)^{\mathbf{2}} + \left(\frac{\mathbf{dT}}{\mathbf{dy}}\right)^{\mathbf{2}} + \left(\frac{\mathbf{dT}}{\mathbf{dz}}\right)^{\mathbf{2}}} \quad (\mathbf{4})$$

Where $\left(\frac{dT}{dx}\right)$, $\left(\frac{dT}{dy}\right)$, $\left(\frac{dT}{dz}\right)$ are the first order derivatives of the magnetic field in the x, y and z directions, respectively.

5.5. Tilt Derivative (TDR):

The tilt derivative filter is a valuable tool in the magnetic data processing and interpretation. It was designed to enhance the visibility of subsurface geological features. This filter is particularly effective in highlighting the subtle anomalies and enhancing the edges of the magnetic sources, making it a crucial technique in various geophysical applications. By dividing the first vertical derivative of the field by the total horizontal derivative of the field, in the X and Y directions, this tilt derivative filter can be calculated [26]. The mathematical formula for this filter is expressed in equation (5):

$$\boldsymbol{TDR} = \frac{\boldsymbol{FVD}}{\boldsymbol{THD}} \quad (\mathbf{5})$$

where FVD is the first vertical derivative (Eq. 2) and THD is the total horizontal gradient of the magnetic field (Eq. 6):

$$\boldsymbol{THD} = \sqrt{\left(\frac{\boldsymbol{dT}}{\boldsymbol{dx}}\right)^{\mathbf{2}} + \left(\frac{\boldsymbol{dT}}{\boldsymbol{dy}}\right)^{\mathbf{2}}} \quad (\mathbf{6})$$

6. RESULTS AND DISCUSSION

6.1. Reduced-to-pole (RTP) map:

The RTP map (figure 2A) shows the occurrence of high magnetic anomalies in the northeastern and western parts of the study area, with average amplitudes from 17 to 122 km and magnitudes of 28 to 110 nT. The low magnetic anomalies exist close to the central parts and at the extreme eastern reaches, with average amplitudes of 50 to 65 km and magnitudes of -162 to -74nT. The high magnetic anomalies indicate shallow depth to the basement rocks while the low magnetic anomalies manifest thick sedimentary cover (i.e. the depth to basement is deep).

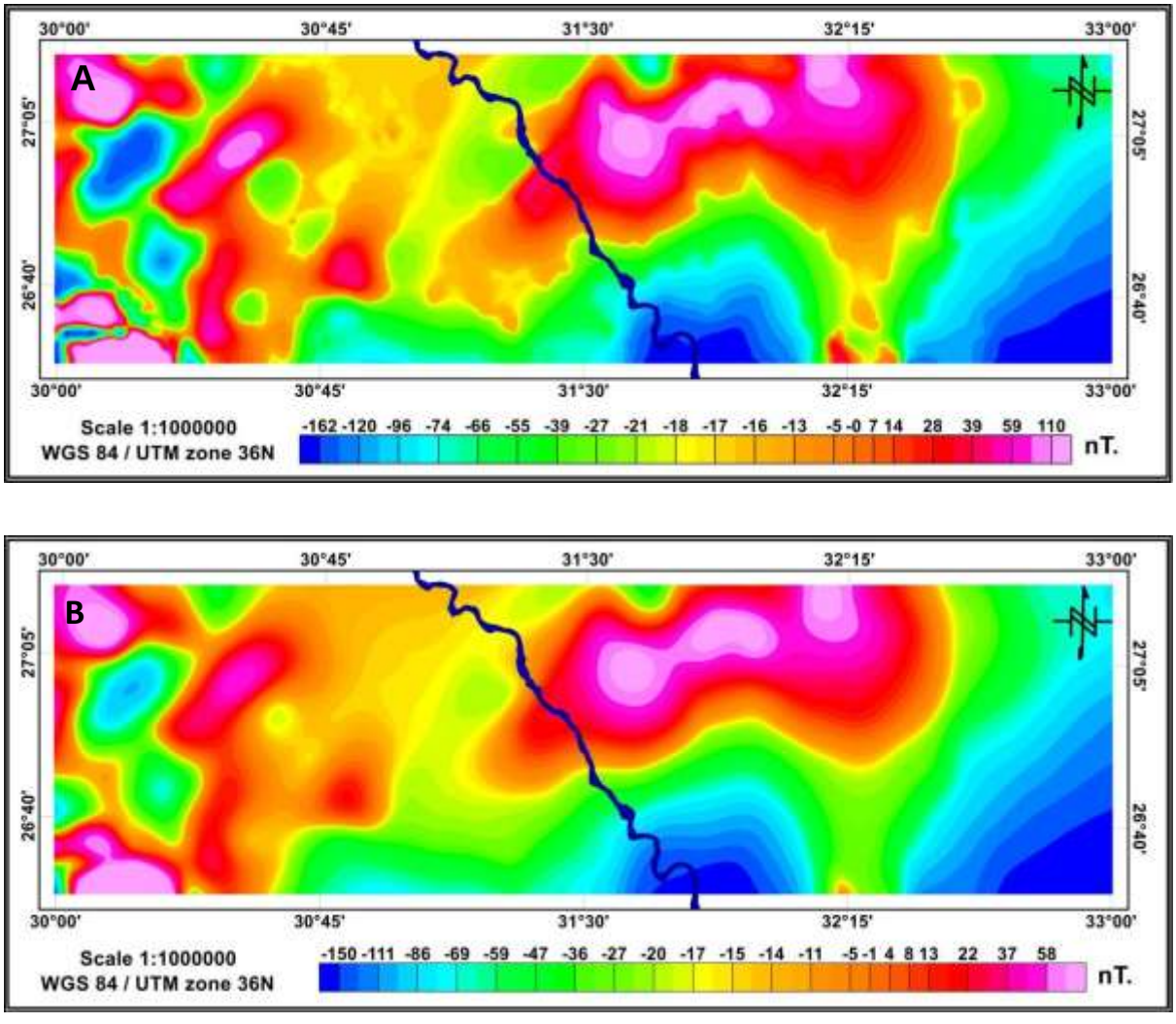

Fig. 2: A) RTP map of the study area, B) Upward continuation map.

6.2. Upward continuation map:

The upward continuation filter is applied to get rid of the high frequency anomalies that disturb the interpretation of the magnetic data and cause the ridging problem. The most suitable upward continuation distance here is 3000 m, because this distance is regarded to have eliminated the high-wavelength noise and, on the meantime, still preserves the original bodies without over-smoothing (Fig. 2B). This map shows the distribution of high bodies in the western parts and near the central zone with average amplitudes of 17 to 51 km and magnitude of 8 to 58 nT., whereas the low bodies are distributed close to the central parts and at the eastern and western areas. The amplitude of these low bodies ranges from 10 to 40 km, with magnitudes of -150 to -70 nT.

6.3. First vertical derivative (FVD):

The FVD map (Fig. 3A) revealed faults throughout the study area, where the zero contour lines indicate structural boundaries between high and low magnetic anomalies and mark the edges between magnetic source bodies (Fig. 3B). These boundaries may be considered to be faults that are traced, analyzed and presented as rose diagram (Fig. 3C). From the diagram, the dominant fault trends are NE-SW followed by the NW-SE trend, however, the E-W trend in low order of predominant.

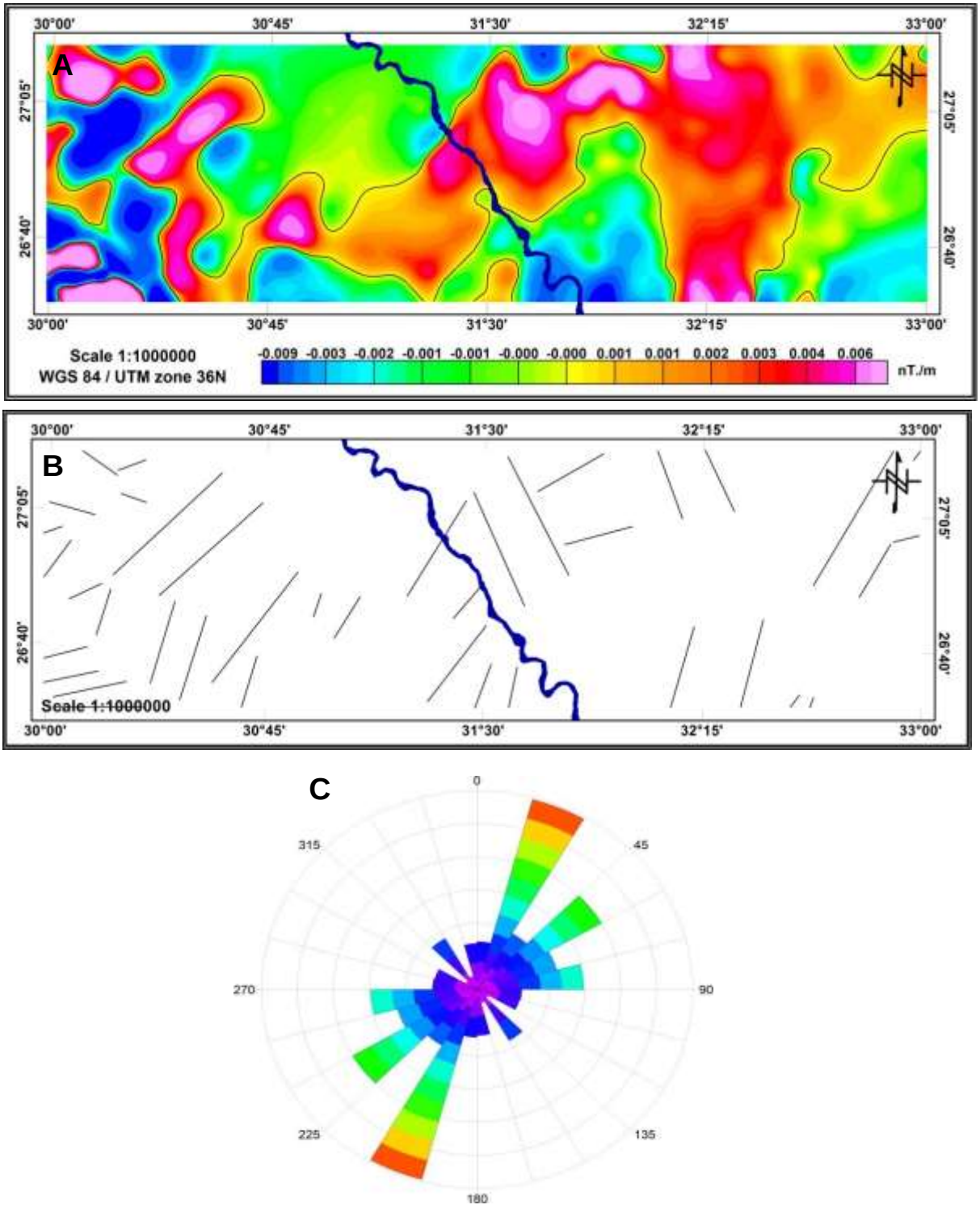

Fig. 3: A) First vertical derivative map (FVD), B) Traced faults based on map 3A, C) Rose diagram of the analyzed major subsurface faults from the FVD filter.

6.4. Butterworth high pass filter:

The output of the Butterworth high pass filter in figure 4A presents the subsurface in a smoother pattern compared to the FVD. The high bodies are intermittent throughout the map at the western, middle and eastern parts. These anomalies have amplitudes range from 16 for the smallest body to 90 km for the largest body. The magnitudes of these bodies measure 2 to 32 nT. The lowest bodies are in the western part of the map, with amplitudes from 12 for the smallest body to 40 km for the largest body. The magnitude for these bodies ranges from -16 to -39 nT. From this map it can be concluded that the main trend of the subsurface faults (Fig. 4B) is the NE-SW trend, and minor faults trends NW-SE and E-W (Fig. 4C).

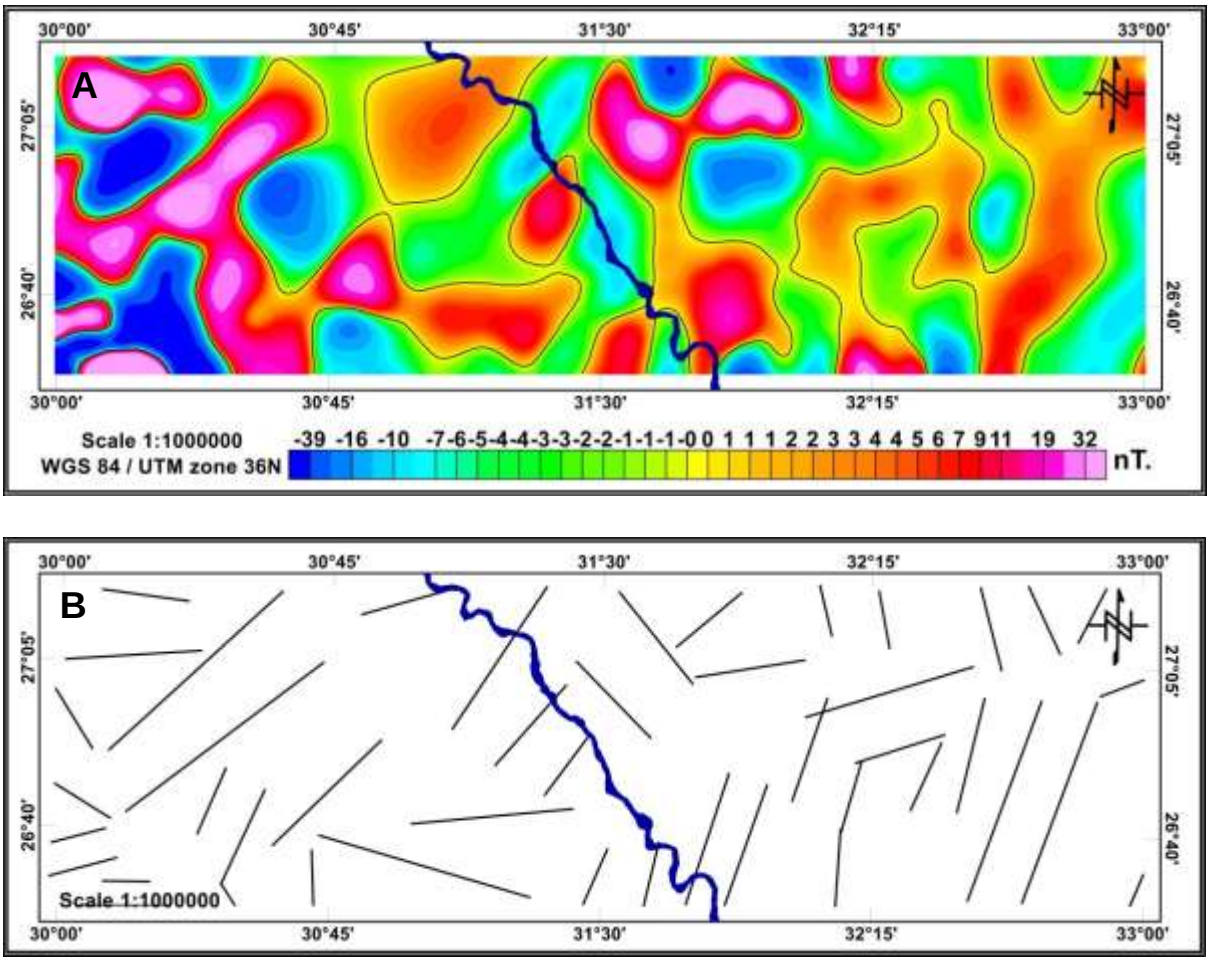

Figure (4): A) Butterworth high pass filter map, B) Traced faults based on map 4A, C) Rose diagram of the analyzed major subsurface faults from the Butterworth high pass filter.

Fig. 4 continued

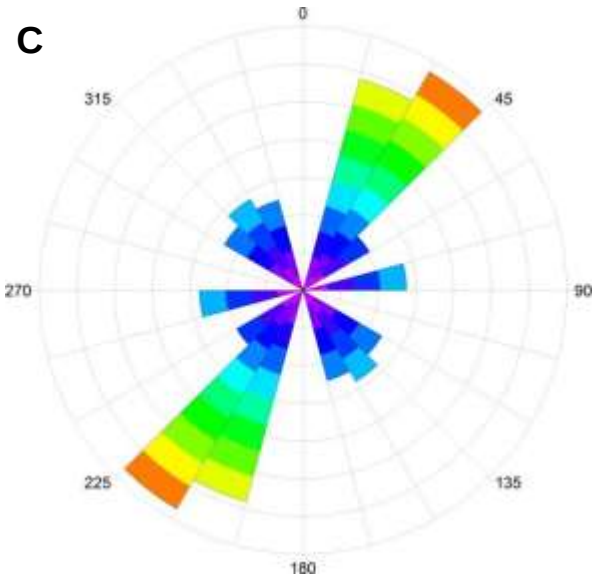

6.5. Analytical Signal filter (AS):

The main advantage of the AS filter is its capacity to identify concealed magnetic bodies and highlight their peripheries. Figure 5A presents the AS filter map, where high magnitudes signify bodies with strong magnetic properties. Mapping the edges of these magnetic bodies corresponds to the mapping of the concealed subsurface faults (Fig. 5B). Figure 5C shows the rose diagram with trends analyzed by the AS filter technique. We established that the main structural trend is the NE-SW; less dominantly the N-NE and NW-SW trends.

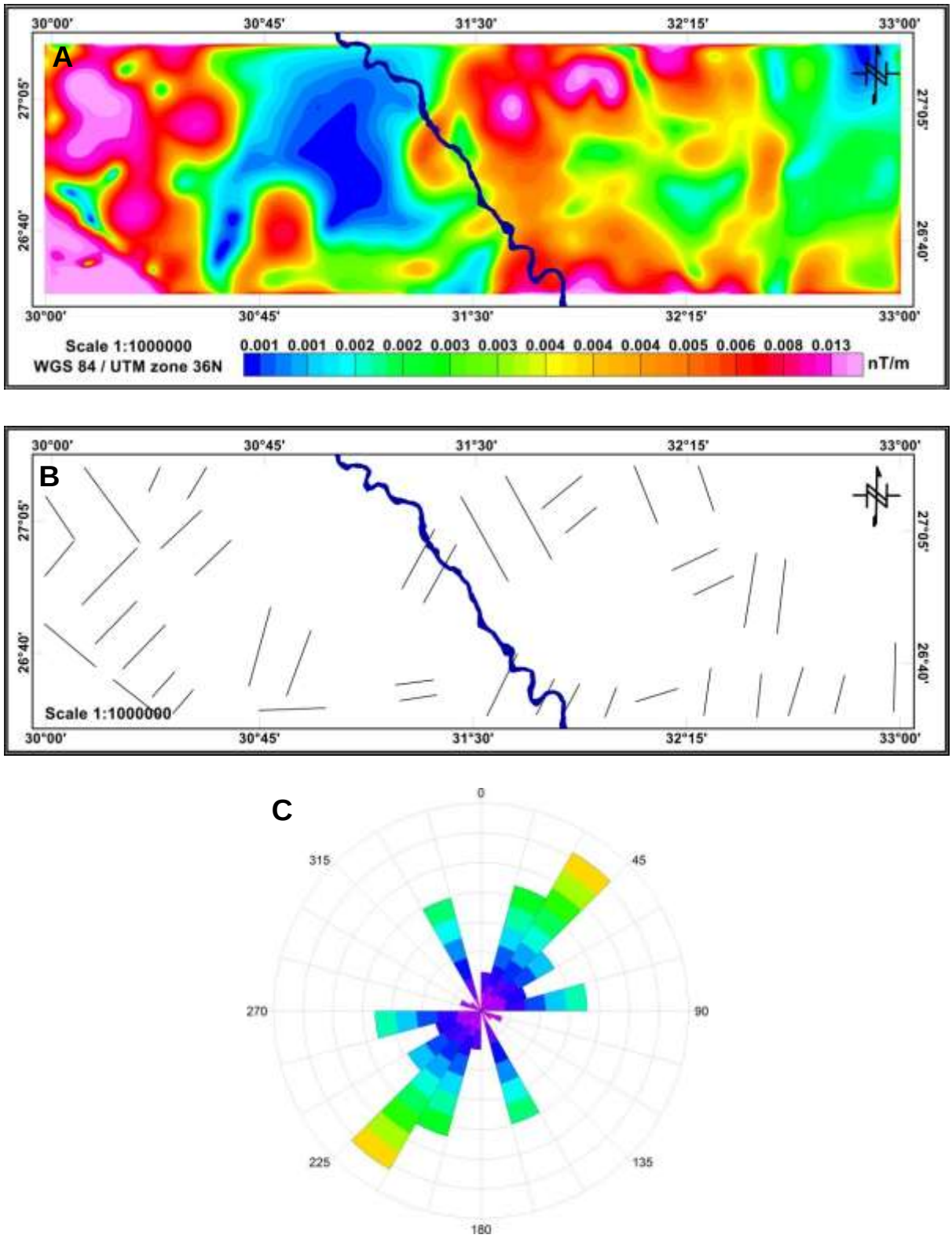

Fig. 5: A) Analytical Signal (AS) filter map, B) Traced faults based on map 5A, C), Rose diagram of the analyzed major subsurface faults from the AS filter.

6.6. Tilt derivative filter (TDR):

The peak values of the TDR filter (Fig. 6A) correspond to the significant subsurface faults (Fig. 6A) with contouring depicting the zero line, which marks the edges of the magnetic bodies (Fig. 6B). The trends of these faults are displayed in the rose diagram of figure 6C, where the main trend is NE-SW.

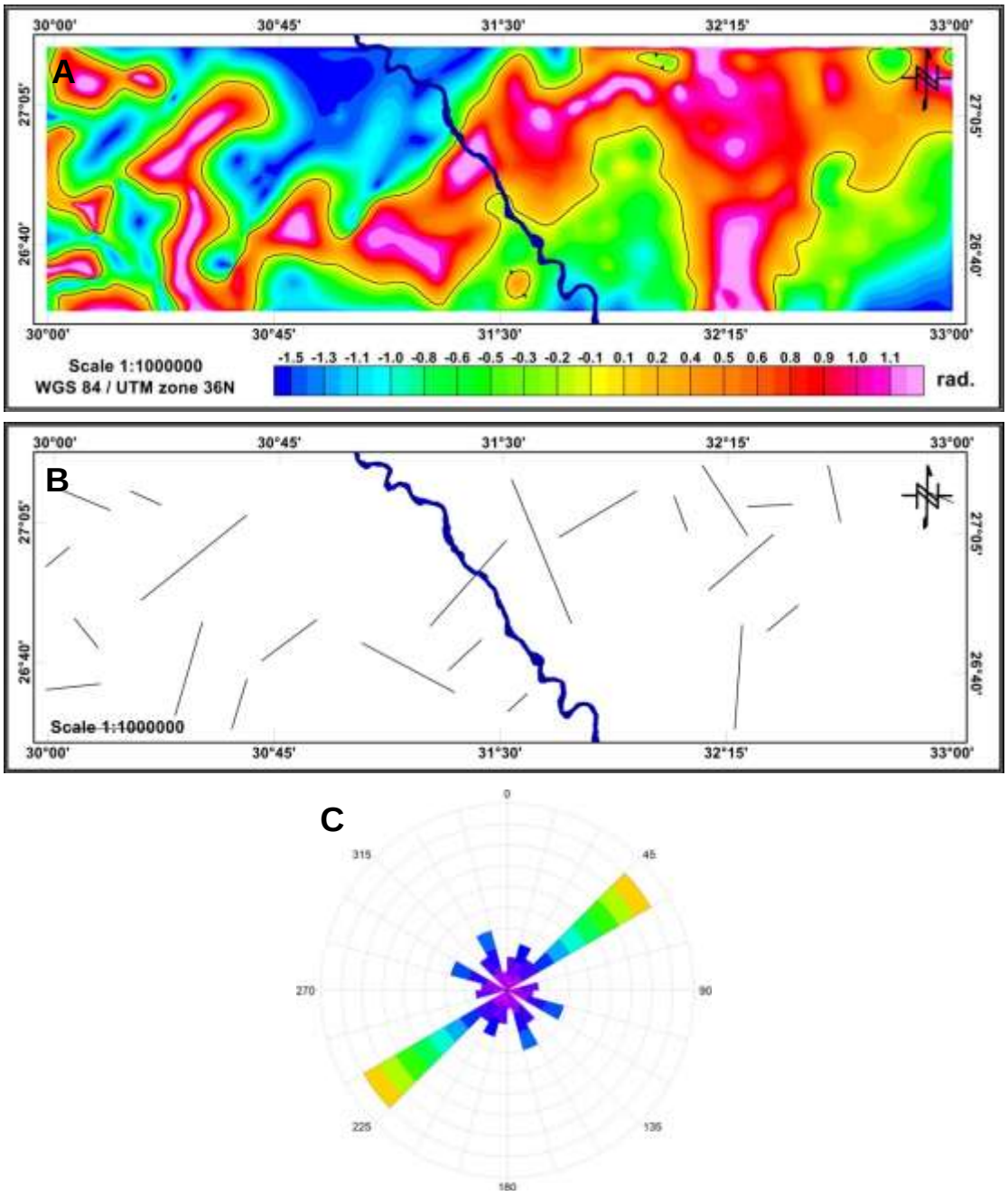

Fig. 6: A) Tilt Derivative filter map (TDR), B) Traced faults based on map 6A, C) Rose diagrams of the analyzed major subsurface faults from the TDR filter

6.7. Surface faults:

The main surface faults in the study area were traced from the geological map of Egypt (Fig. 7), published by the Egyptian Geological Survey and Mining Authority [19]. These faults were categorized and plotted on the rose diagram of figure 7B, where the predominant faults are extending in the NW-SE direction.

In conclusion, the processing and interpretation of the aeromagnetic data reveal that the major subsurface fault trends frequently extend mainly in a NE-SW direction. In contrast, the surface faults are extending in a NW- SE direction. By correlating the subsurface and surface fault trends a great discrepancy is observed, indicating no continuity. Consequently, such non continuity suggests no hydrogeological connection between the aquifer systems in the study area. This conclusion implies that the shallow CAS in the study area does not receive substantial recharge from the NSAS. This hypothesis of the absence of a significant recharge from the NSAS is supported by the results of [27], through isotopic analyses of groundwater samples representing the two aquifer systems. In that work of [27], the highly isotopically depleted samples, that are clearly indicative of recharge from the NSAS, are found outside the present study area, namely in Wadi El Assiuty. After the construction of the Aswan High Dam, the water experiences longer resting times that boosts the enrichment of such isotopic signature because of the longer evaporation times than the past [28]. On the other hand, samples from the Eocene Aquifer are isotopically slightly depleted, implying no significant recharge from the NSAS towards the Eocene Aquifer; they are rather indicative of horizontal recharge from the Nile water before the construction of Aswan High Dam.

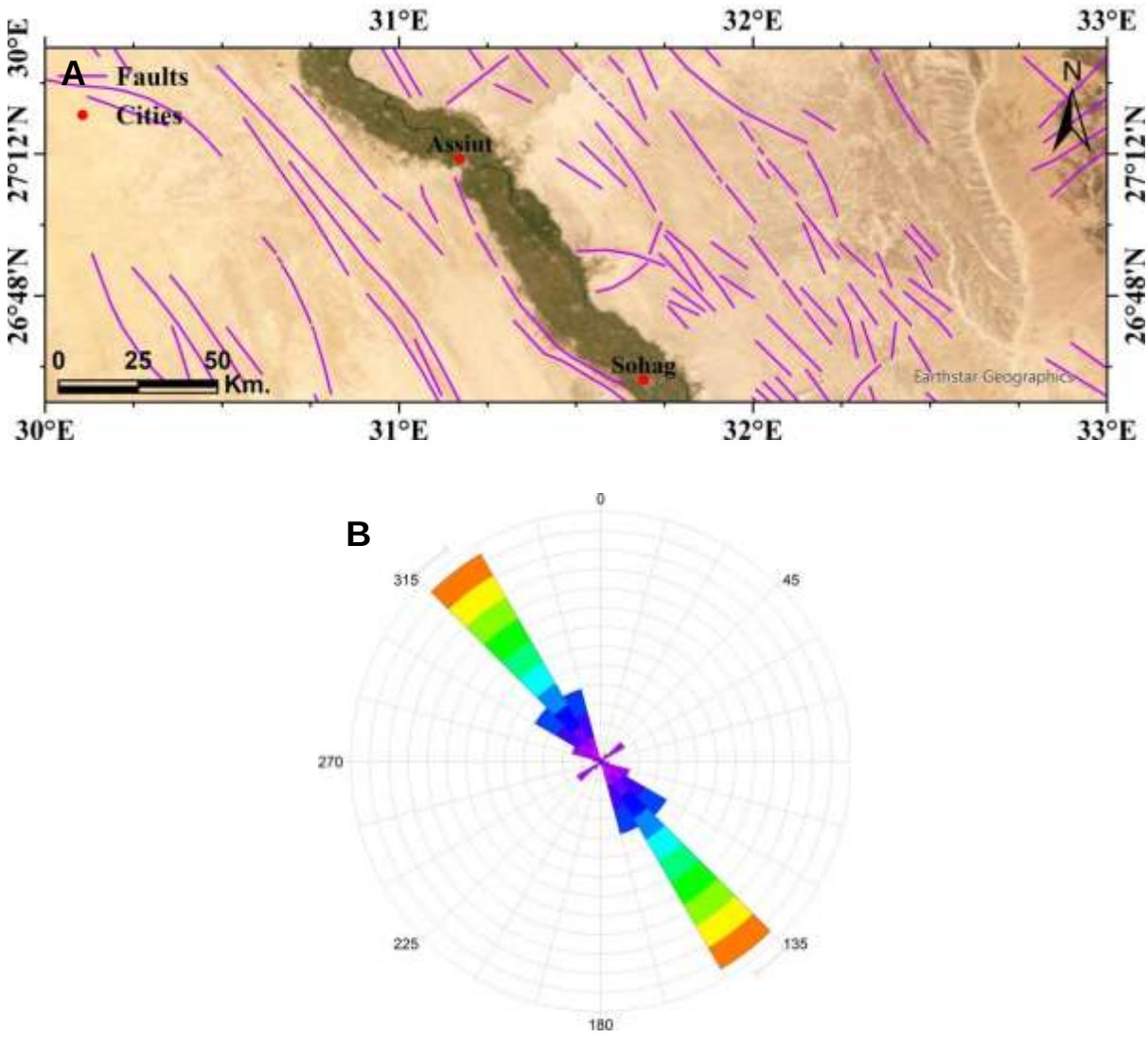

Fig. 7: A) Map showing major surface faults after EGSMA (1981), B) Rose diagram of the analyzed major surface faults of map 7A.

7. CONCLUSION

From the above discussion, the following concluding remarks can be highlighted:

1- The deep subsurface fault trends run mainly northeast-southwest (NE-SW), in contrast to the surface faults trend, which runs northwest-southeast (NW-SE).

2- This demonstrated discontinuity between the subsurface and surface fault trends favors no possibility of a hydrogeological connectivity between the deep NSAS and SCAS, at least in the study area.

3- Water recharging is therefore not expected from the deep NSAS groundwater aquifer to the shallow SCAS, in order to compensate for the heavy extraction rate of the latter. In this case any reclamation projects based on the groundwater of the SCAS as a source of water is risky.

4- Additional research on the present area beyond this aeromagnetic study (e.g. geophysical, isotopical and borehole data) is recommended as supplementary information to address this important issue, which directs future planning of reclamation projects.

ACKNOWLEDGEMENTS

We would like to express my sincere gratitude to the editor for his valuable guidance and support throughout the review process. I am also deeply appreciative of the insightful comments and constructive suggestions provided by the two anonymous reviewers, which have enhanced the manuscript.

REFERENCES

[1]. S. A. Araffa, S. Bedair, Application of Land Magnetic and Geoelectrical Techniques for Delineating Groundwater Aquifer: Case Study in East Oweinat, Western Desert, Egypt. Nat.l Res. Res., 30 (2021), 4219–4233. https://doi.org/10.1007/s11053-021-09937-y

[2]. H. R. Burger, A. F. Sheehan, and C. H. Jones, Introduction to Applied Geophysics: Exploring the Shallow Subsurface. Cambridge: Cambridge University Press, 2023.

[3]. J. Milsom, Field Geophysics, 3rd ed. Wiley, 2003.

[4]. E. Custodio, "Aquifer overexploitation: what does it mean?," Hydrogeology Journal, vol. 10, 2002, pp. 254–277. https://doi.org/10.1007/s10040-002-0188-6

[5]. T. Gleeson, Y. Wada, M. Bierkens, et al., "Water balance of global aquifers revealed by groundwater footprint," Nature, vol. 488, 2012, pp. 197–200. https://doi.org/10.1038/nature11295

[6]. J. Famiglietti, "The global groundwater crisis," Nature Climate Change, vol. 4, 2014, pp. 945–948. https://doi.org/10.1038/nclimate2425

[7]. V. Bense, T. Gleeson, S. Loveless, O. Bour, and J. Scibek, "Fault zone hydrogeology," Earth- Science Reviews, vol. 127, 2013, pp. 171-192. https://doi.org/10.1016/j.earscirev.2013.09.008

[8]. H. Chen, Q. Niu, A. Mendieta, J. Bradford, and J. McNamara, "Geophysics- Informed Hydrologic Modeling of a Mountain Headwater Catchment for Studying Hydrological Partitioning in the Critical Zone," Water Resources Research, vol. 59, 2023. https://doi.org/10.1029/2023WR035280

[9]. C.W. Fetter, Applied Hydrogeology, 3rd ed. Macmillan College Publishing Company, New York, 1994.

[10]. F. Gori, M. Paternoster, M. Barbieri, D. Buttitta, A. Caracausi, F. Parente, A. Sulli, and M. Petitta, "Hydrogeochemical multi-component approach to assess fluids upwelling and mixing in shallow carbonate-evaporitic aquifers (Contursi area, southern Apennines, Italy)," Journal of Hydrology, vol. 618, 2023, p. 129-258, https://doi.org/10.1016/j.jhydrol.2023.129258

[11]. Conoco Coral (1987) Geological Map of Egypt, Cairo, Egypt, NG 36 NW Asyut sheet, Scale 1:500,000.

[12]. M.H. El-Azabi and S. Farouk, "A Standard Sequence Stratigraphic Scheme for the Maastrichtian-Ypresian Successions of the Southern and Central Western Desert, Egypt," in The Phanerozoic Geology and Natural Resources of Egypt, Z. Hamimi et al., Eds., Advances in Science, Technology & Innovation, Springer, Cham, 2023. https://doi.org/10.1007/978-3-030-95637-0_13

[13]. M. H. El-Azabi and S. Farouk, "High-resolution sequence stratigraphy of the Maastrichtian- Ypresian succession along the eastern scarp face of Kharga Oasis, southern Western Desert, Egypt," Sedimentology, vol. 58, no. 3, 2011, pp. 579–617. https://doi.org/10.1111/j.1365-3091.2010.01175.x

[15]. U. Thorweihe, "Nubian Aquifer system," in The Geology of Egypt, 1990, pp. 601–611. https://doi.org/10.1201/9780203736678-28

[16]. M. Sultan, E. Yan, N. Sturchio, A. Wagdy, K. Abdel Gelil, R. Becker, N. Manocha, and A. Milewski, "Natural discharge: A key to sustainable utilization of fossil groundwater," Journal of Hydrology, vol. 335, no. 1–2, pp. 25–36, 2007. https://doi.org/10.1016/j.jhydrol.2006.10.034

[17]. M.R. El Tahlawi, A.A. Farrag, and S.S. Ahmed, "Groundwater of Egypt: An environmental overview," Environmental Geology, vol. 55, no. 3, 2008, pp. 639–652. https://doi.org/10.1007/s00254-007-1014-1

[17]. M. El-Rawy, F. Abdalla, and M. El Alfy, "Water Resources in Egypt," in The Geology of Egypt, Z. Hamimi, A. El-Barkooky, J. Martínez Frías, H. Fritz, and Y. Abd El-Rahman, Eds., Regional Geology Reviews, Springer, Cham, 2020. https://doi.org/10.1007/978-3-030-15265-9_18

[18]. V. Baranov, "A new method for interpretation of aeromagnetic maps: Pseudo-gravimetric anomalies," GEOPHYSICS, vol. 22, no. 2, 1957. http://library.seg.org/

[19]. Egyptian Geological Survey and Minning Authority (EGSMA) (1981). GEOLOGICAL MAP OF EGYPT, scale 1: 2,000,000.

[20]. Geosoft Inc. (2015). Oasis montaj (Version 8.4) [Computer software].

[21]. V. Baranov, "A new method for interpretation of aeromagnetic maps; pseudo-gravimetric anomalies" Geophysics, vol. 22, no. 2, pp. 359–382. https://doi.org/10.1190/1.1438369

[22]. W. J. Hinze, R. R. B. von Frese, and A. H. Saad, Gravity and Magnetic Exploration: Principles, Practices, and Applications, Cambridge University Press, 2013.

[23]. R. J. Blakely, Potential Theory in Gravity and Magnetic Applications, 1995. https://doi.org/10.1017/CBO9780511549816

[24]. S. Butterworth, "On the theory of filter amplifiers," Wireless Engineer, vol. 7, 1930. pp. 536- 541.

[25]. M. N. Nabighian, "The analytic signal of two-dimensional magnetic bodies with polygonal cross-section: Its properties and use for automated anomaly interpretation," Geophysics, vol. 37, no. 3, 2012, pp. 507–517. https://doi.org/10.1190/1.1440276

[26]. B. Verduzco, J. D. Fairhead, C. M. Green, and C. MacKenzie, "New insights into magnetic derivatives for structural mapping," Geophysics, vol. 23, no. 2, 2012, pp. 116–119. https://doi.org/10.1190/1.1651454

[27]. E. A. Korany, R. N. Tempel, M. A. Gomaa, and R. G. Mohamed, "Detecting the roles of the physio-chemical processes on groundwater evolution, Assiut area, Egypt-applications of hydrogeochemical and isotopic approaches," Egyptian Journal of Geology, vol. 57, pp. 63-83, 2013.

[28] A. El Bakri, A. Tantawi, B. Blavoux, and M. Dray, Sources of water recharge identified by isotopes in El Minya governate (Nile Valley, Middle Egypt). International Atomic Energy Agency (IAEA). 1992